Neuron
Article

VEGF Mediates Commissural Axon Chemoattraction through Its Receptor Flk1

Carmen Ruiz de Almodovar,[1,2,16] Pierre J. Fabre,[3,16] Ellen Knevels,[1,2] Cathy Coulon,[1,2] Inmaculada Segura,[1,2] Patrick C.G. Haddick,[4] Liesbeth Aerts,[1,2] Nicolas Delattin,[1,2] Geraldine Strasser,[4] Won-Jong Oh,[5] Christian Lange,[1,2] Stefan Vinckier,[1,2] Jody Haigh,[6,7] Coralie Fouquet,[8] Chengua Gu,[5] Kari Alitalo,[9,10,11,12] Valerie Castellani,[13] Marc Tessier-Lavigne,[4] Alain Chedotal,[14] Frederic Charron,[3,15,*] and Peter Carmeliet[1,2,*]

[1]VIB
[2]KULeuven
Laboratory for Angiogenesis and the Neurovascular link, Vesalius Research Center (VRC), KULeuven, Leuven, Belgium
[3]Molecular Biology of Neural Development, Institut de Recherches Cliniques de Montreal (IRCM) and Department of Medicine, University of Montreal, Montreal QC H2W 1R7, Canada
[4]Genentech, South San Francisco, San Francisco, CA 94080, USA
[5]Department of Neurobiology, Harvard Medical School, Boston, MA 02115, USA
[6]Vascular Cell Biology Unit, Department for Molecular Biomedical Research, VIB, Ghent, Belgium
[7]Department for Molecular Biomedical Research, UGent, Ghent, Belgium
[8]CNRS UMR7102, UPMC-Paris 6, 75005 Paris, France
[9]Molecular/Cancer Biology Program, Biomedicum Helsinki
[10]Department of Pathology, Haartman Institute
[11]Institute for Molecular Medicine Finland
[12]Helsinki University Central Hospital
University of Helsinki, Helsinki FIN-00014, Finland
[13]University of Lyon 1, Claude Bernard Lyon 1, CGMC, UMR, CNRS, F-69000 Lyon, France
[14]Department of Development, INSERM, UMR_S968, Institut de la Vision, F-75012 Paris, France
[15]Department of Anatomy and Cell Biology, Department of Biology, Division of Experimental Medicine and Program in Neuroengineering, McGill University, Montreal QC H3A 2B2, Canada
[16]These authors contributed equally to this work
*Correspondence: frederic.charron@ircm.qc.ca (F.C.), peter.carmeliet@vib-kuleuven.be (P.C.)
DOI 10.1016/j.neuron.2011.04.014

SUMMARY

Growing axons are guided to their targets by attractive and repulsive cues. In the developing spinal cord, Netrin-1 and Shh guide commissural axons toward the midline. However, the combined inhibition of their activity in commissural axon turning assays does not completely abrogate turning toward floor plate tissue, suggesting that additional guidance cues are present. Here we show that the prototypic angiogenic factor VEGF is secreted by the floor plate and is a chemoattractant for commissural axons in vitro and in vivo. Inactivation of *Vegf* in the floor plate or of its receptor *Flk1* in commissural neurons causes axon guidance defects, whereas Flk1 blockade inhibits turning of axons to VEGF in vitro. Similar to Shh and Netrin-1, VEGF-mediated commissural axon guidance requires the activity of Src family kinases. Our results identify VEGF and Flk1 as a novel ligand/receptor pair controlling commissural axon guidance.

INTRODUCTION

During developmental wiring of the nervous system, axons respond to attractive and repulsive guidance cues to navigate to their targets. Surprisingly, only a small number of guidance cues have been identified so far, suggesting that additional chemoattractants and repellents remain to be discovered. A well-known model system to study axon guidance is the spinal cord ventral midline. During development, commissural neurons, located in the dorsal spinal cord, send axons that project toward and subsequently across the floor plate, a specialized structure at the ventral midline, which acts as an intermediate target and influences commissural axons by expressing attractive and repulsive cues (Dickson and Zou, 2010).

The first midline guidance cue identified, Netrin-1, has two distinct activities on precrossing commissural axons: it stimulates growth and attracts these axons toward the floor plate (reviewed in Charron and Tessier-Lavigne, 2005). Precrossing commissural axons are also guided by Sonic hedgehog (Shh), which chemoattracts commissural axons without stimulating their growth (Charron et al., 2003). Although Shh and Netrin-1 are required for normal guidance of commissural axons, intriguingly, when dorsal spinal cord explants are exposed to Netrin-1-deficient floor plates in the presence of Shh signaling inhibitors, some commissural axons are still attracted (Charron et al., 2003). This suggests that the floor plate secretes other chemoattractants than Netrin-1 and Shh. However, the molecular nature of these floor plate-derived attractant guidance cues remains unknown.

Increasing evidence indicates that vascular endothelial growth factor A (VEGF-A, termed VEGF from hereon), a prototypic

angiogenic factor, plays a key role in the nervous system (Ruiz de Almodovar et al., 2009). For instance, VEGF promotes proliferation, migration, differentiation and survival of neuroblasts (Jin et al., 2002; Wittko et al., 2009; Zhang et al., 2003), and induces axonal outgrowth of various neurons (Ruiz de Almodovar et al., 2009). By activating its signaling receptor Flk1, VEGF chemoattracts cerebellar granule cells (Ruiz de Almodovar et al., 2010). VEGF also regulates neuronal migration via binding to Neuropilin-1 (Npn1) (Schwarz et al., 2004). Initially discovered to bind some class 3 Semaphorins (Sema), Npn1 was later identified as a coreceptor of Flk1 (also termed VEGF receptor-2) that binds VEGF as well (Schwarz and Ruhrberg, 2010; Soker et al., 1998). Ligation of VEGF to Npn1 controls migration of somata of facial branchio-motor neurons, whereas interaction of Sema3A with a Npn1/PlexinA4 complex guides their axons (Schwarz et al., 2004, 2008). Flk1 also regulates axon outgrowth of neurons from the subiculum on binding of Sema3E to a Npn1/PlexinD1 complex that activates Flk1 in the absence of VEGF (Bellon et al., 2010). However, whether VEGF can function as an axonal chemoattractant remains unknown.

Here, we show that VEGF is expressed and secreted by the floor plate during commissural axon guidance, that mice lacking a single *Vegf* allele in the floor plate exhibit commissural axon guidance defects and that VEGF attracts commissural axons in vitro. We also show that the VEGF receptor Flk1 is expressed by commissural neurons and that its inhibition blocks the chemoattractant activity of VEGF in vitro. Moreover, genetic inactivation of *Flk1* in commissural neurons causes axonal guidance defects in vivo. Finally, we show that VEGF stimulates Src-family kinase (SFK) activity in commissural neurons and that SFK activity is required for VEGF-mediated chemoattraction. Taken together, our findings that VEGF acts via Flk1 as a floor plate chemoattractant for commissural axons identify a novel ligand/receptor pair controlling commissural axon guidance.

RESULTS

VEGF Is Expressed at the Floor Plate

Commissural axon chemoattractants, such as Netrin-1 and Shh, are expressed by the floor plate at the time when these axons project ventrally to the midline (Kennedy et al., 2006; Roelink et al., 1995). Netrin-1 is also expressed in the periventricular zone of the neural tube in a dorsoventral gradient (Kennedy et al., 2006; Serafini et al., 1996). Previous studies showed that VEGF is expressed at the floor plate and motor columns of the developing spinal cord at embryonic day (E)8.5–E10.5 (Hogan et al., 2004; James et al., 2009; Nagase et al., 2005), but expression at the floor plate at later stages when commissural axons cross the midline has not been analyzed. We first used in situ hybridization (ISH) to analyze VEGF mRNA expression in the spinal cord (Figures 1A and 1B). At E11.5, when commissural axons project ventrally to the midline, a VEGF signal was clearly detectable at the floor plate (Figure 1A). In addition, a weaker signal was also present in motor neurons and the ventral two thirds of the periventricular zone of the neural tube (Figure 1A).

To confirm the ISH data, we also used a VEGF-LacZ reporter line ($Vegf^{LacZ}$). In this strain, an IRES-LacZ reporter cassette has been knocked into the noncoding region of the last exon of the

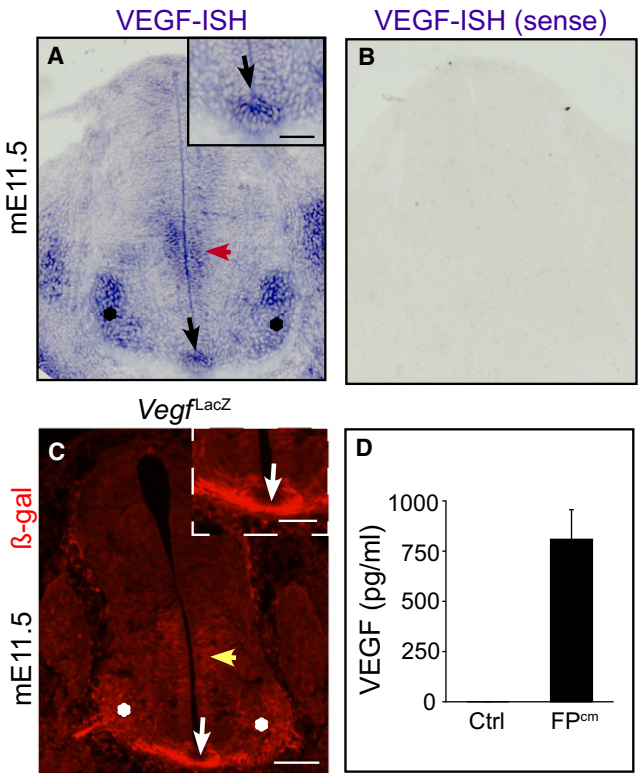

Figure 1. VEGF Is Expressed at the Floor Plate

(A) In situ hybridization of VEGF mRNA on a E11.5 mouse spinal cord transverse section showing expression of VEGF at the floor plate (black arrow; also shown at higher magnification in inset), in the ventral spinal cord (red arrow), and in the motor columns (asterisks).

(B) A sense probe, used as negative control, did not give any background signal.

(C) β-Gal immunostaining (red) of a E11.5 $VEGF^{LacZ}$ mouse spinal cord transverse section at low and high (inset) magnification, revealing expression of β-Gal in the ventral spinal cord (yellow arrow), motor columns (asterisks), and floor plate (white arrow).

(D) Bar graphs showing VEGF protein levels (mean ± standard error of the mean [SEM]), released in floor plate conditioned medium (FP^{cm}) from E11.5 WT mouse embryos, but not in control medium (Ctrl). Scale bars represent 100 μm (A–C); 50 μm (insets, A and C).

Vegf gene (Miquerol et al., 2000). Because this line expresses LacZ from the endogenous *Vegf* gene locus, the spatio-temporal expression pattern of the β-galactosidase (β-Gal) marker reliably mimics that of the endogenous *Vegf* mRNA (Miquerol et al., 1999; Ruiz de Almodovar et al., 2010; Storkebaum et al., 2010). In accordance with the ISH results, β-Gal immunostaining and enzymatic staining (X-gal) of spinal cord cross-sections from E11.5 $Vegf^{LacZ}$ mouse embryos revealed a clear signal at the floor plate (Figure 1C; see Figure S1A available online) and a weaker signal in motor neurons and the ventral two-thirds of the periventricular zone of the neural tube (Figure 1C; Figure S1A).

To test whether VEGF was secreted, we microdissected floor plates from E11.5 mouse embryos, cultured them individually, and analyzed their conditioned medium by ELISA. These individual floor plate explant cultures released detectable levels of VEGF in the conditioned medium (Figure 1D). For comparison,

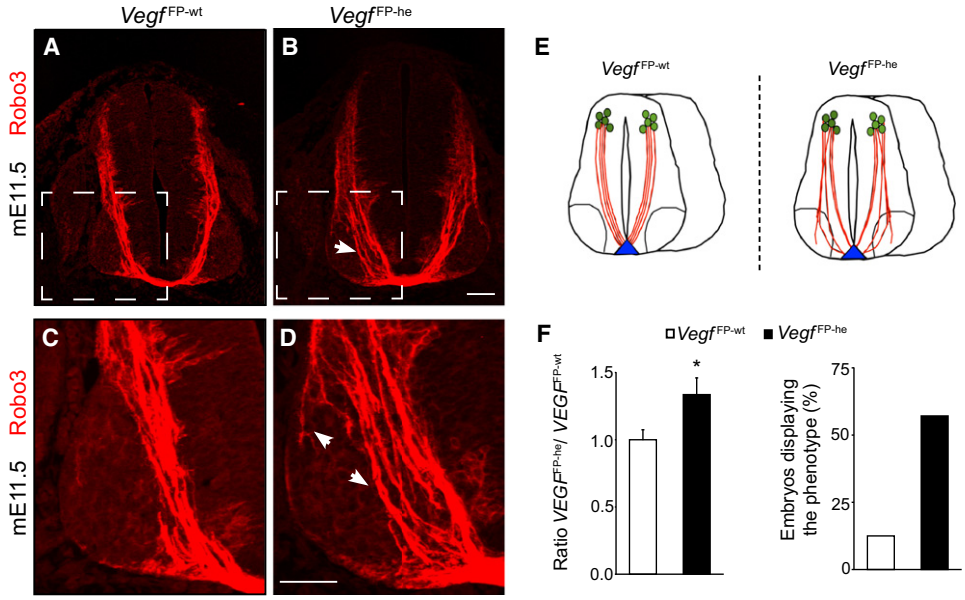

Figure 2. Inactivation of VEGF in the Floor Plate Causes Axon Guidance Defects In Vivo

(A–D) Robo3 immunostaining (red) in embryos with inactivation of one allele of *Vegf* in the floor plate (*Vegf*$^{FP\text{-}he}$; generated by crossing Hoxa1-Cre with *Vegf*$^{lox/lox}$ mice) and in control embryos (*Vegf*$^{FP\text{-}wt}$). Compared to *Vegf*$^{FP\text{-}wt}$ embryos (A) and (C), commissural axons in *Vegf*$^{FP\text{-}he}$ embryos are defasciculated and some axons project near the lateral edge of the spinal cord (white arrows) (B) and (D). (C) and (D) are higher magnification of the insets in (A) and (B).

(E) Scheme depicting the observed phenotypes. Left: normal commissural axons (red) project from the dorsal spinal cord to the floor plate (blue) in *Vegf*$^{FP\text{-}wt}$ embryos. Right: in *Vegf*$^{FP\text{-}he}$ embryos, axons project in a highly disorganized and defasciculated manner.

(F) Left: histogram shows the quantification of the area occupied by commissural axons (% of total spinal cord area), normalized to the values obtained in *Vegf*$^{FP\text{-}wt}$ embryos (mean ± SEM; see Experimental Procedures). *p = 0.03, Student's t test; n = 8 *Vegf*$^{FP\text{-}wt}$ and n = 7 *Vegf*$^{FP\text{-}he}$. Right: histogram showing the penetrance of the axon guidance phenotype (%); n = 8 *Vegf*$^{FP\text{-}wt}$; n = 7 *Vegf*$^{FP\text{-}he}$. Scale bars represent 100 μm (A and B); 20 μm (C and D).

released Shh levels in the same conditioned media were 22.7 ± 4.2 pg/ml (n = 7). RT-PCR analysis of freshly microdissected floor plates from E11.5 mice confirmed the production of mRNA transcripts (expressed as mRNA copies/10^5 mRNA copies β-actin (mean ± standard error of the mean [SEM]; n = 5) for VEGF (35 ± 1), Shh (81 ± 2), and Netrin-1 (358 ± 37). Thus, VEGF is produced and secreted by the floor plate during the developmental window when commissural axons are chemoattracted to the midline.

Floor Plate VEGF Is Required for Commissural Axon Guidance In Vivo

Heterozygous VEGF deficient (*Vegf*$^{+/-}$) mice die early during embryonic development ~E9.0–E9.5 due to severe vascular malformations and thus cannot be used for later analysis of commissural axon guidance at the midline (Carmeliet et al., 1996; Ferrara et al., 1996). Thus, in order to analyze the role of floor plate-derived VEGF in commissural axon guidance, we inactivated *Vegf* specifically in the floor plate by crossing the Hoxa1-Cre driver line with mice carrying a floxed *Vegf* allele (Gerber et al., 1999). In this line, the Cre recombinase is expressed in the floor plate of the spinal cord to about rhombomere level 5 in the hindbrain (C.F. and A.C., unpublished data) (Li and Lufkin, 2000). In accordance with previous findings that deficiency of a single VEGF allele can already cause phenotypic defects (Carmeliet et al., 1996; Ferrara et al., 1996), most of Hoxa1-Cre$^{(+)}$;*Vegf*^{loxlox} embryos were growth-retarded, exhibited abnormal development, and did not survive till E11.5 (the precise reason of the lethality remains to be further determined). We therefore analyzed commissural axon navigation at E11.5 in Hoxa1-Cre$^{(+)}$;*Vegf*$^{lox/wt}$ (*Vegf*$^{FP\text{-}he}$) embryos, carrying one wild-type and one inactivated allele, and in their corresponding Hoxa1-Cre$^{(-)}$;*Vegf*$^{lox/wt}$ (*Vegf*$^{FP\text{-}wt}$) littermates. PCR analysis confirmed correct excision of the floxed *Vegf* allele in *Vegf*$^{FP\text{-}he}$ embryos (data not shown).

We first confirmed that VEGF secretion was lower in floor plates from *Vegf*$^{FP\text{-}he}$ than *Vegf*$^{FP\text{-}wt}$ embryos. Measurements of VEGF protein levels secreted in the conditioned media by individual floor plates indeed revealed that VEGF secretion by *Vegf*$^{FP\text{-}he}$ floor plates was reduced as compared to *Vegf*$^{FP\text{-}wt}$ floor plates (pg/ml: 809 ± 147 for *Vegf*$^{FP\text{-}wt}$ versus 344 ± 93 for *Vegf*$^{FP\text{-}he}$; n = 7–3; p = 0.02). When expressed relative to the protein levels of Shh in the conditioned media, the VEGF/Shh ratio was also lower in *Vegf*$^{FP\text{-}he}$ than *Vegf*$^{FP\text{-}wt}$ mice (37.7 ± 7.0 in *Vegf*$^{FP\text{-}wt}$ versus 12.4 ± 4.3 in *Vegf*$^{FP\text{-}he}$; mean ± SEM, n = 7–3; p = 0.015).

Immunostaining of spinal cord cross-sections from *Vegf*$^{FP\text{-}he}$ embryos for Robo3 to identify precrossing commissural axons revealed that these axons exhibited abnormal pathfinding, were defasciculated and projected to the lateral edge of the ventral spinal cord (Figures 2A–2E). Such aberrant commissural axon pathfinding was rarely observed in *Vegf*$^{FP\text{-}wt}$ control embryos (Figures 2A and 2C). Quantitative analysis confirmed that the area occupied by Robo3$^+$ axons was larger and that these

guidance defects were more frequent in *Vegf*$^{FP\text{-}he}$ than *Vegf*$^{FP\text{-}wt}$ embryos (Figure 2F). Thus, floor plate-derived VEGF is necessary for normal guidance of precrossing spinal commissural axons in vivo. The commissural axon guidance defects in *Vegf*$^{FP\text{-}he}$ embryos were not secondary to altered expression of Netrin-1 or Shh, because ISH analysis at E11.5 showed that the pattern and level of expression of Netrin-1 and Shh were comparable in *Vegf*$^{FP\text{-}he}$ and *Vegf*$^{FP\text{-}wt}$ embryos (Figures S2A–S2D).

Commissural Neurons Express VEGF Receptor Flk1

Because VEGF signals via Flk1 to regulate cerebellar granule cell migration (Ruiz de Almodovar et al., 2010) and axon outgrowth (Ruiz de Almodovar et al., 2009), we assessed whether commissural neurons expressed this receptor. It is well established that neurons express Flk1 at much lower levels than endothelial cells, rendering in situ detection of Flk1 in neurons challenging (Ruiz de Almodovar et al., 2009, 2010; Storkebaum et al., 2005). Nonetheless, genetic and pharmacological loss- and gain-of-function studies established that Flk1 signals important biological processes in neurons (Bellon et al., 2010; Ruiz de Almodovar et al., 2009, 2010). In fact, it has been postulated that this differential expression of VEGF receptors allows VEGF to exert effects on neurons without inducing angiogenesis (Storkebaum et al., 2005; Zacchigna et al., 2008). To maximize detection of Flk1 expression in neurons, we used a panel of techniques.

We first determined the expression of Flk1 in precrossing commissural axons by taking advantage of anti-Flk1 antibodies (#SC6251 and #SC504) that detect Flk1 selectively in neurons but not in endothelial cells, presumably because of different posttranslational modifications of the receptor in these different cell types (Marko and Damon, 2008; Ruiz de Almodovar et al., 2010; Storkebaum et al., 2010). Spinal cord sections from E13 rat embryos (corresponding to E11.5 in mouse embryos) were double-immunostained for Flk1 and Robo3, using a sensitive detection method. This analysis confirmed the expression of low levels of Flk1 in Robo3^{+} precrossing commissural axons in vivo (Figures 3A–3L).

Finally, we microdissected dorsal spinal cord tissue from E13 rat embryos, as this tissue contains a highly enriched population of commissural neurons (Langlois et al., 2010; Yam et al., 2009). RT-PCR and ELISA confirmed that Flk1 was expressed at the mRNA (0.19 ± 0.05 copies Flk1 mRNA/10^3 copies β-actin, n = 3) and protein level (0.2 ng Flk1 per mg protein; measurement on a pool of three samples, each containing ~10 embryos). Moreover, we purified commissural neurons from E13 rat embryos and, after 16 hr in culture, double-immunostained them for Flk1 and either Robo3 or TAG-1 (another marker of precrossing commissural axons). This analysis confirmed that commissural neurons express Flk1 (Figures 3M–3R). Quantification revealed that the large majority (93%, n = 138) of commissural neurons coexpressed TAG-1 and Flk1. Taken together, these results indicate that precrossing commissural axons express low levels of Flk1, capable of binding VEGF.

VEGF Chemoattracts Commissural Axons In Vitro via Flk1

To assess whether VEGF can directly chemoattract commissural axons, we analyzed the response of commissural axons to a gradient of VEGF using the Dunn chamber axon guidance assay (Yam et al., 2009). Purified commissural neurons isolated from E13 rat embryos, which express Flk1 (see above), were exposed to a control (buffer containing BSA) or a VEGF gradient. Commissural axons continued to grow without any deviation from their original trajectory when exposed to a control gradient (Figures 4A–4C and 4E), but actively turned toward the VEGF gradient (Figures 4A, 4B, 4D, and 4E; Movie S1). Even axons with growth cones oriented nearly in the opposite direction of the VEGF gradient were able to turn toward the VEGF gradient (Figures 4B and 4D). When measuring the turning response of these axons, a significant positive turning (attraction) was observed within 1.5 hr of VEGF gradient formation (Figure 4E), indicating that VEGF is a chemoattractant for commissural axons.

To assess which receptor mediated the chemoattractive effect of VEGF, we performed turning experiments in the presence of receptor-neutralizing antibodies. Consistent with Flk1 being the receptor mediating the guidance activity of VEGF on commissural axons, VEGF-mediated chemoattraction was completely abolished when Flk1 was blocked by a neutralizing anti-Flk1 monoclonal antibody (Figure 4E). Although Npn1 can modulate axonal growth and neuronal migration (Cheng et al., 2004; Schwarz et al., 2004), we and others failed to detect expression of Npn1 in commissural neurons (Figure S1B) (Chen et al., 1997). To exclude the possibility that very low levels of Npn1 (e.g., below the detection threshold) could contribute to the chemo-attractive effect of VEGF, we also performed Npn1 antibody-blocking experiments. In contrast to inhibiting Flk1, blockage of Npn1 had no significant effect on the ability of VEGF to attract commissural axons in vitro (Figure 4E). Taken together, these results indicate that VEGF chemoattracts commissural axons through Flk1.

Flk1 Is Required for Commissural Axon Guidance In Vivo

To analyze whether Flk1 also functionally regulated commissural axon guidance in vivo, we inactivated *Flk1* specifically in commissural neurons by crossing *Flk1*$^{lox/LacZ}$ mice with the Wnt1-Cre driver line, which induces Cre-mediated recombination in commissural neurons in the dorsal spinal cord (Charron et al., 2003). We and others previously described that intercrossing *Flk1*$^{lox/lox}$ mice with various Cre-driver lines resulted only in incomplete inactivation of Flk1 (Maes et al., 2010; Ruiz de Almodovar et al., 2010). In order to increase the efficiency of Flk1 excision and to obtain complete absence of Flk1 in commissural neurons, we intercrossed Wnt1-Cre mice with *Flk1*$^{lox/LacZ}$ mice that carry one floxed and one inactivated *Flk1* allele in which the *LacZ* expression cassette replaces the first exons of *Flk1* (Ema et al., 2006). PCR analysis confirmed that the floxed *Flk1* allele was correctly inactivated in the spinal cord from E11.5 Wnt1-Cre$^{(+)}$;*Flk1*$^{lox/LacZ}$ embryos (referred to as *Flk1*$^{CN\text{-}ko}$ embryos) (data not shown).

Spinal cord sections from E11.5 *Flk1*$^{CN\text{-}ko}$ embryos immunostained for Robo3 revealed that precrossing commissural axons exhibited abnormal pathfinding, projected to the lateral edge of the ventral spinal cord, invaded the motor columns and were defasciculated (Figures 5A–5G). Such aberrant axon pathfinding was only very rarely observed in control E11.5 Wnt1-Cre$^{(-)}$;*Flk1*$^{lox/LacZ}$ (*Flk1*$^{CN\text{-}wt}$) embryos, which still express

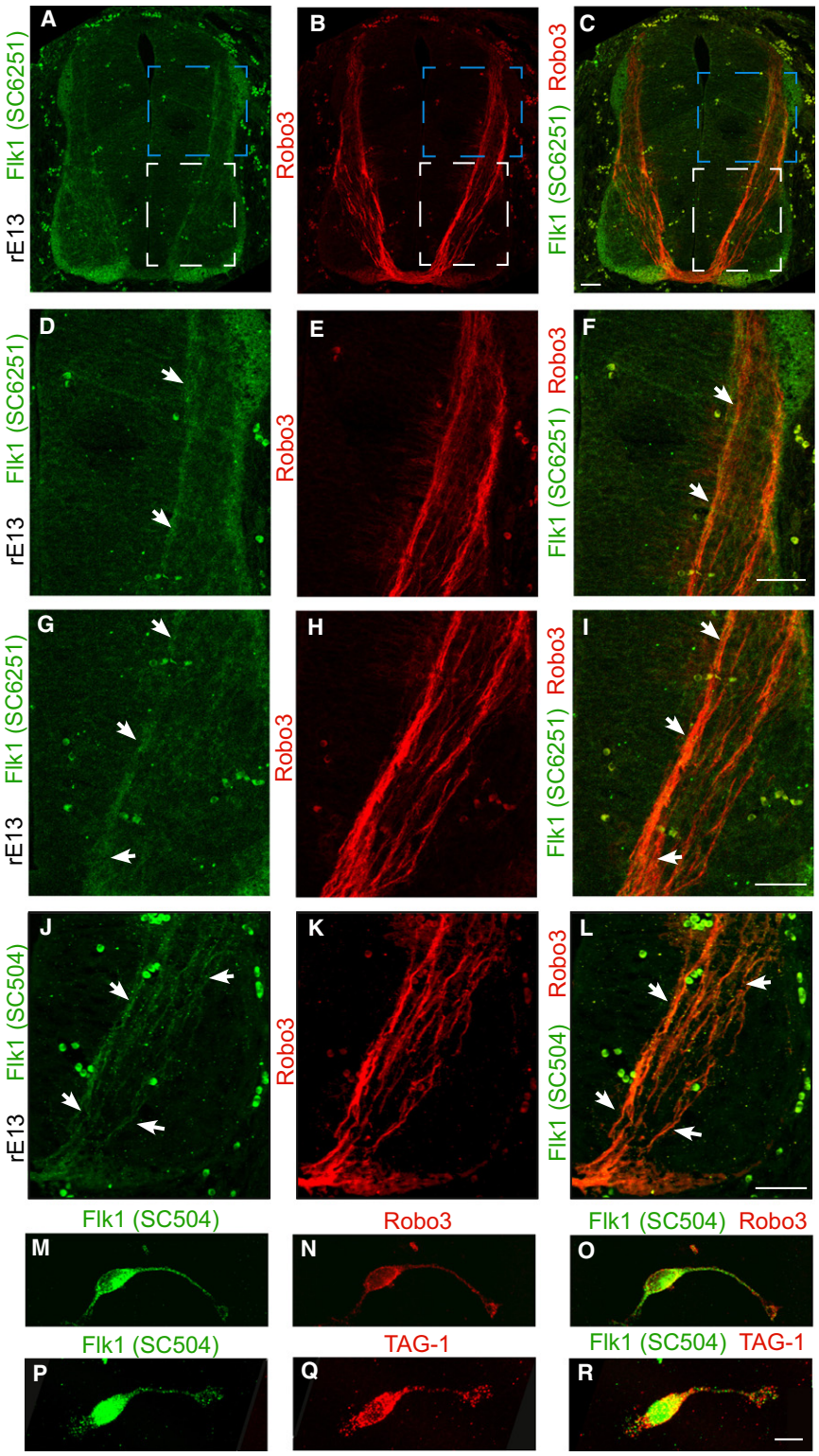

Figure 3. Flk1 Is Expressed in Commissural Neurons

(A–L) Double immunostaining for Flk1 (A, D, G, and J: green) and Robo3 (B, E, H, and K: red) in E13 rat embryo sections using two different anti-Flk1 antibodies known to label Flk1 in neurons (#SC6251 [A–I] and #SC504 [J–L]), showing Flk1 expression in pre- and postcrossing commissural axons; (C), (F), (I), and (L) show the merged images. (D)–(F) and (G)–(I) are higher magnification of the blue and white insets, respectively, shown in (A)–(C). The arrows (D, F, G, I, J, and L) point to Flk1^{+} commissural axons.

(M–R) Double immunostaining for Flk1 (green in M and P) and Robo3 (red in N) or TAG-1 (red in Q) in dissociated commissural neurons showing expression of Flk1 in the cell body, axon and growth cone of commissural neurons; (O) and (R): merged images. Scale bars represent 50 μm (A–L); 10 μm (M–R).

functional Flk1 (Figures 5A, 5D, and 5G). Morphometric analysis confirmed that the area occupied by Robo3^{+} axons was significantly larger and that these guidance defects were more frequent in *Flk1*$^{CN\text{-}ko}$ than *Flk1*$^{CN\text{-}wt}$ embryos (Figure 5H). Similar to what we found in *Vegf*$^{FP\text{-}he}$ mouse embryos, the pattern and level of expression of Netrin-1 and Shh were comparable between *Flk1*$^{CN\text{-}ko}$ and their corresponding wild-type littermates (Figures S3A–S3D), indicating that Flk1 cell-autonomously controls guidance of precrossing commissural axons in vivo.

Other VEGF Homologs and Flk1-Ligands Are Redundant with VEGF-A

To assess how specific the role of VEGF and Flk1 in commissural axon guidance is, we analyzed the expression and role of additional VEGF homologs that can bind to murine Flk1 (VEGF-C) or indirectly activate Flk1 (Sema3E) (see Introduction). ISH revealed that VEGF-C was not expressed at the floor plate or ventral spinal cord at the time of commissural axon guidance (Figure S1C). In addition, VEGF-C did not induce turning of commissural axons in the Dunn chamber assay (Figure S4A). Consistent with these in vitro findings, homozygous VEGF-C deficiency did not cause commissural axon guidance defects in vivo (data not shown).

Through binding Npn1/PlexinD1, which forms a signaling complex with Flk1, Sema3E is capable of activating Flk1 independently of VEGF (Bellon et al., 2010). Sema3E is expressed at the floor plate at the time of midline crossing (Figure S1D), but was found not to be required for pre- or postcrossing commissural axon outgrowth (Zou et al.,

2000), but its possible role in guidance of precrossing commissural axons was never investigated. However, a Sema3E gradient failed to induce turning of commissural axons in the Dunn chamber turning assay (Figure S4A). Altogether, these results suggest that Flk1-dependent commissural axon guidance in vivo does not occur via Sema3E and that VEGF, but not VEGF-C, is the guidance cue responsible for this effect.

Src Family Kinase Activity Is Required for VEGF-Mediated Axon Guidance

Floor plate-derived guidance cues such as Netrin-1 and Shh induce local changes at the growth cone in a transcriptionally independent manner (Li et al., 2004; Yam et al., 2009). In particular, Src family kinases (SFKs) are expressed by commissural neurons and activated in their growth cones (Yam et al., 2009). Moreover, SFKs are known to participate in the guidance of axons by Netrin-1 and Shh (Li et al., 2004; Yam et al., 2009), whereas VEGF stimulates endothelial cell migration via SFK activation (Eliceiri et al., 2002; Olsson et al., 2006). Because of all these reasons, we explored whether SFKs also participated in VEGF-mediated axon guidance. Notably, VEGF stimulation of isolated commissural neurons elevated the levels of active SFKs, as measured by immunoblotting when using an antibody specifically recognizing the phosphorylated tyrosine residue Y418 in SFKs (Figure 6A). Moreover, immunostaining revealed that SFKs were activated in the growth cone (Figure 6B). Morphometric quantification revealed that VEGF, at concentrations that induced axon turning, increased the levels of phospho-SFKs in commissural neuron growth cones (Figure 6B).

We next tested whether activation of SFKs is required for VEGF-mediated axon guidance. We therefore exposed commissural neurons in the Dunn chamber to a gradient of VEGF in the presence of PP2 (a widely used SFK inhibitor) or its inactive analog (PP3). Analysis of growth cone turning revealed that neurons in the presence of PP3 turned normally in response to VEGF (Figures 6C, 6D, and 6F). However, when neurons were exposed to a VEGF gradient in the presence of PP2, axons did no longer turn toward the VEGF gradient (Figures 6C, 6E, and 6F). Altogether, these results indicate that VEGF activates SFKs in commissural neurons and that SFK activity is required for VEGF-mediated commissural axon guidance.

DISCUSSION

In order to reach the floor plate, commissural axons need to grow and navigate from the dorsal to the ventral spinal cord. Whereas Netrin-1 seems to account for the majority of the growth-promoting activity of the floor plate (Serafini et al., 1996), chemoattraction of precrossing commissural axons to the floor plate is controlled by both Netrin-1 and Shh (Charron et al., 2003). In the present study, we identified VEGF as an additional commissural axon chemoattractant at the floor plate.

Our findings indicate that the prototypic endothelial growth factor VEGF is an axonal chemoattractant. VEGF is expressed at the floor plate and ventral spinal cord at the time when commissural axons navigate to the midline, reminiscent of the spatio-temporal expression pattern of Netrin-1 and Shh, i.e., other guidance cues for commissural axons (Dickson and Zou, 2010). VEGF is not only detectable at the mRNA level, but is also released by floor plate cells into the extracellular milieu. Similarly to Shh (Yam et al., 2009), VEGF induces commissural axon turning in the Dunn chamber. Furthermore, loss-of-function of *Vegf* at the floor plate induced commissural axon guidance defects, indicating that it has a nonredundant activity as a guidance cue. Its importance in this process is further supported by findings that inactivation of only a single *Vegf* allele already sufficed to cause navigation defects. VEGF is well known to have gene dosage-dependent effects and haplo-insufficient phenotypes in vascular development have been documented (Carmeliet et al., 1996; Ferrara et al., 1996). Moreover, even reductions of VEGF levels by less than 50% suffice to impair neuronal survival or migration (Oosthuyse et al., 2001; Ruiz de Almodovar et al., 2010).

This guidance effect of VEGF on commissural axons is mediated by Flk1. Indeed, Flk1 is expressed by purified commissural neurons in vitro and detectable at low levels by various complementary methods in precrossing commissural axons in the developing spinal cord in vivo. Furthermore, a neutralizing anti-Flk1 antibody completely blocked the VEGF-mediated chemoattraction of commissural axons in the Dunn chamber. Moreover, inactivation of *Flk1* in commissural neurons using the Wnt1-Cre driver line showed that Flk1 is essential for commissural axon guidance in vivo. When *Flk1* was inactivated, commissural axon trajectories were defective. Many axons failed to turn appropriately toward the ventral midline as they entered the ventral spinal cord, and instead projected aberrantly and invaded the motor columns. Because the Wnt1-Cre driver does not induce recombination in the ventral spinal cord (Charron et al., 2003), these results suggest a cell-autonomous requirement for Flk1 signaling in commissural axon guidance in vivo. Overall, the observed phenotype was similar to the one observed in floor plate-specific heterozygous VEGF deficient mice. Based on the expression of VEGF at the floor plate and on the ability of VEGF to attract commissural axons in a Flk1-dependent manner in vitro, we propose that, in vivo, commissural axons lacking *Flk1* exhibit pathfinding errors and deviate from their normal trajectory because of a failure to detect the floor plate chemoattractant VEGF. Of interest, *Flk1*-mutant commissural axons also exhibit a defasciculated phenotype in the ventral spinal cord. Whether fasciculation of commissural axons is an additional Flk1-dependent effect distinct from its effect in mediating axon turning needs further investigation.

Interestingly, floor plate-specific *Vegf* haplodeficient and commissural neuron-specific *Flk1* null embryos display a phenotype that is similar to that of embryos lacking the Shh receptor *Boc* or of embryos with conditional inactivation of the Shh signaling component *Smoothened* (*Smo*) in commissural neurons (Charron et al., 2003; Okada et al., 2006). Indeed, in these mutant embryos, precrossing commissural axons were able to reach the midline, but occupied a larger area in the ventral spinal cord and invaded the motor columns, thus showing primarily a guidance defect and not an axonal growth defect. Also, the magnitude of the in vitro turning effect of VEGF is comparable to that of Shh (Yam et al., 2009). Loss-of-function of VEGF did not, however, alter the expression pattern and levels of Netrin-1 or Shh, further supporting the concept that Flk1

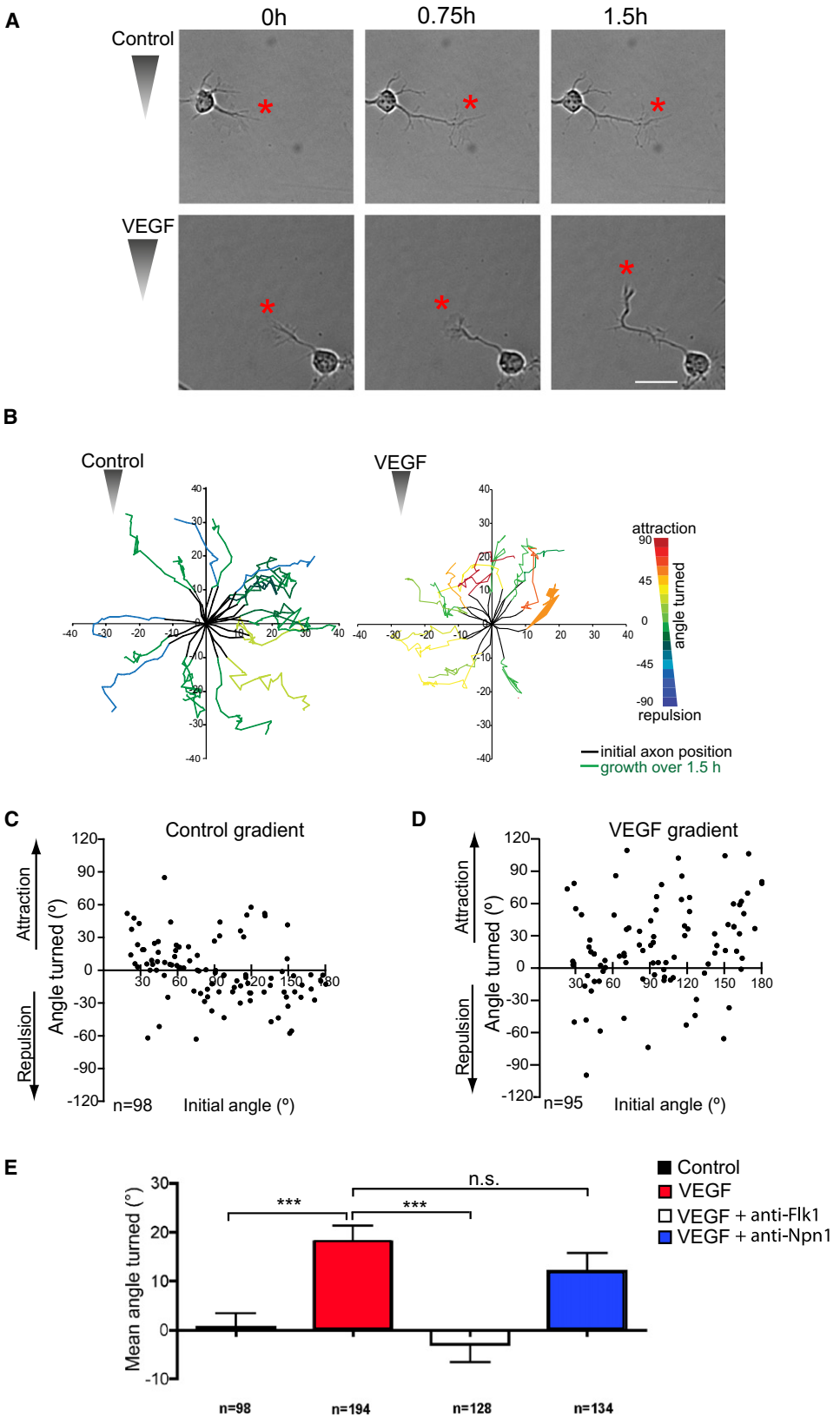
A
0h
0.75h
1.5h
Control
VEGF
B
Control
VEGF
attraction
angle turned
repulsion
initial axon position
growth over 1.5 h
C
Control gradient
Attraction
Repulsion
Angle turned (°)
n=98
Initial angle (°)
D
VEGF gradient
Attraction
Repulsion
Angle turned (°)
n=95
Initial angle (°)
E
Mean angle turned (°)
***
***
n.s.
Control
VEGF
VEGF + anti-Flk1
VEGF + anti-Npn1
n=98
n=194
n=128
n=134

transmits the VEGF guidance cue signals directly to commissural axons. SKFs are key players in the regulation of growth cone dynamics and cytoskeleton rearrangement (Liu et al., 2007; Robles et al., 2005) and graded SFK activity in the growth cone is known to mediate axon turning, with growth cones turning toward the side of higher SFK activity (Robles et al., 2005; Yam et al., 2009). Interestingly, similar as two other floor plate-derived guidance cues, i.e., Netrin-1 and Shh (Liu et al., 2004, 2007; Meriane et al., 2004; Yam et al., 2009), VEGF also chemoattracts commissural axons via activation of SFKs in their growth cones. This may suggest a model whereby distinct molecular guidance cues utilize the same intracellular signaling machinery (e.g., SFKs) to generate an integrated navigation response to the midline.

Similar to Shh, VEGF was unable to induce outgrowth of E13 rat dorsal spinal cord explants (Figure S5B–S5E) and, if anything, slightly reduced axonal extension of purified commissural neurons in the Dunn chamber assay (Figure S5F). The lack of a growth-promoting effect of VEGF on precrossing commissural axons differs from its ability to promote axonal outgrowth of superior cervical and dorsal root ganglia, cortical neurons and retinal ganglion cells (Böcker-Meffert et al., 2002; Jin et al., 2002; Rosenstein et al., 2003; Sondell and Kanje, 2001; Sondell et al., 1999) and suggests cell-type specific contextual activities for VEGF.

Previous studies documented that VEGF can affect wiring of the brain in a context-dependent pattern via effects on Npn1 (Schwarz et al., 2004). In accordance with previous findings that failed to detect Npn1 in commissural neurons (Chen et al., 1997), a neutralizing Npn1 blocking antibody was ineffective in blocking the VEGF induced commissural axons turning in the Dunn chamber assay. Moreover, we could not find any evidence that VEGF-C, another ligand of Flk1 (Lohela et al., 2009) or Sema3E, another ligand of Npn1 that indirectly activates Flk1 signaling in other types of neurons (Bellon et al., 2010), control commissural axon navigation. VEGF-D, another ligand of Flk1 in humans but not in mice (Baldwin et al., 2001), is not expressed in the ventral spinal cord (Avantaggiato et al., 1998). Thus, VEGF chemoattracts commissural axons through Flk1, with a negligible or redundant role for other Flk1 ligands (VEGF-C) or activators (Sema3E), or VEGF receptors (Npn1).

Curiously, motor columns express *Vegf* mRNA, yet neither vessels nor commissural axons invade these structures (James et al., 2009). It is possible that motor neurons make the *Vegf* message (mRNA), but do not secrete the protein from their cell body, and target it to their axonal compartment (as is thought to occur for *Slit2*; M.T.-L. and A. Jaworski, unpublished data). Another alternative explanation is that additional signals prevent blood vessels and commissural axons from entering the motor columns.

VEGF was originally discovered as a key angiogenic factor. Only subsequent studies revealed that this factor can affect neurons directly, independently of its angiogenic activity (Rosenstein et al., 2010; Ruiz de Almodovar et al., 2009, 2010; Tam and Watts, 2010). In the developing spinal cord, VEGF orchestrates the formation of the neurovascular plexus and subsequent vessel sprouting from this plexus into the avascular neural tube (James et al., 2009). Interestingly, however, even though vascularization of the neural tube occurs at the same time as commissural axon midline crossing, our conditional *Flk1* inactivation studies in commissural neurons and in vitro turning assays establish that VEGF chemoattracts these axons independently of any VEGF-related vascular activity. To the best of our knowledge, this is the first report documenting an angiogenesis-independent effect of VEGF on axon guidance.

EXPERIMENTAL PROCEDURES

Animals

The *VEGF*^{LacZ} mouse line was kindly provided by A. Nagy and was previously described (Miquerol et al., 1999). VEGF-C knockout mice were previously described (Karkkainen et al., 2004), and the *VEGF*$^{lox/lox}$ mouse line was kindly provided by D. Anderson and previously described (Gerber et al., 1999). The transgenic Wnt1-Cre mouse line was kindly provided by A. McMahon. The transgenic Hoxa1-Cre mouse line was generated by A. Chedotal using a previously described cDNA (Li and Lufkin, 2000). The *Flk1*$^{lox/LacZ}$ mouse line was generated by crossing *Flk1*$^{lox/lox}$ mice (Haigh et al., 2003) with *Flk1*$^{LacZ/+}$ mice (Maes et al., 2010). For each transgenic line, WT littermate embryos were used. Wistar or Sprague Dawley rat embryos (E13) were used for explant outgrowth assays, purification of commissural neurons and for immuno-histochemistry. All animals were treated according to the guidelines approved by the Animal Care Committees of the K.U.Leuven (Belgium) and of the IRCM (Canada).

Commissural Neuron Culture

Commissural neurons were prepared from the dorsal fifth of E13 rat neural tubes as described (Langlois et al., 2010; Yam et al., 2009). Purified commissural neurons were plated on poly-Lysine coated coverslips (for immunostaining) or square 3D coverslips (for Dunn chamber assay) at low density in neurobasal medium supplemented with 10% FBS and 2 mM L-Glutamine (Invitrogen). After 20 hr, the medium was replaced with Neurobasal medium, supplemented with 2% B27 (Invitrogen) and 2 mM L-Glutamine. Commissural neurons were then used for the Dunn chamber axon guidance assay (40 hr after plating) or fixed for immunostaining (30 hr after plating).

Histology and Immunohistochemistry

Mouse and rat embryos were dissected and fixed with 4% paraformaldehyde (PFA) overnight at 4°C (mouse embryos) or 2 hr at room temperature (rat embryos). Transverse serial cryosections of dissected embryos were cut at

Figure 4. VEGF Induces Commissural Axon Turning in a Flk1-Dependent Manner

(A) Representative images of commissural neurons subjected to a control gradient (BSA, top) or a VEGF gradient (25 ng/ml, bottom) showing no change of direction in commissural axons exposed to the control gradient (red asterisks in top), but a significant turning toward increasing concentrations of VEGF in neurons exposed to a VEGF gradient (red asterisks in bottom) over the course of 1.5 hr. Increasing gradient concentrations (from bottom to top) are represented by a wedge. Scale bar represents 20 μm.

(B) Trajectory plots of a sample of 20 axons in control (left) or 16 axons in 25 ng/ml VEGF (right) gradient. All trajectories have been rotated so that the gradient increases along the y axis. The initial axon position is shown in black and the axon growth over 1.5 hr is colored according to the angle turned (scale is shown on the right).

(C and D) Scatter plots of the angle turned versus initial angle for commissural axons in a control (C) or a VEGF gradient (25 ng/ml in the outer well) (D).

(E) Histogram representing the mean angle turned (±SEM) for initial angles >20° in response to a control gradient (black bar), a VEGF gradient (25 ng/ml; red bar), a VEGF gradient (25 ng/ml) in the presence of anti-Flk1 (100 ng/ml) (white bar), or a VEGF gradient (25 ng/ml) in the presence of anti-Npn1 (10 μg/ml) (blue bar) (one way ANOVA with Bonferroni posttest, ***$p < 0.001$; ns: not significant).

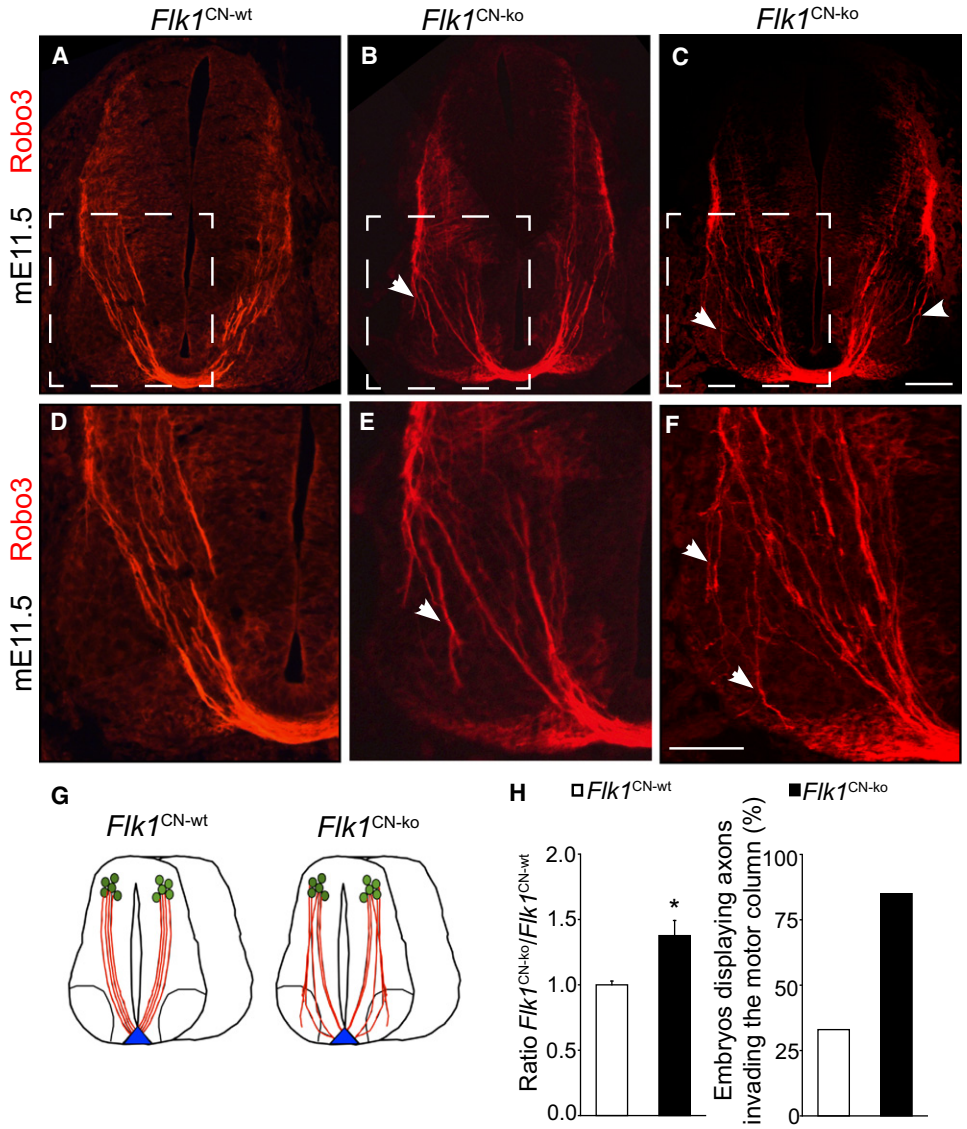

Figure 5. Inactivation of Flk1 Causes Commissural Axon Guidance Defects In Vivo

(A–F) Robo3 immunostaining (red) in embryos with selective inactivation of *Flk1* in the dorsal spinal cord ($Flk1^{CN\text{-}ko}$; generated by crossing Wnt-1-Cre with $Flk1^{lox/LacZ}$ mice) and in control embryos ($Flk1^{CN\text{-}wt}$). Compared to $Flk1^{CN\text{-}wt}$ embryos (A and D), commissural axons in $Flk1^{CN\text{-}ko}$ embryos are defasciculated and some axons project near the lateral edge of the spinal cord and invade the motor columns (white arrows) (B, C, E, and F). (D–F) Higher magnification of the insets in (A–C). (B) and (E) and (C) and (F) are representative images from two different mutant embryos.

(G) Scheme depicting the observed phenotype. Left: normal commissural axons (red) project from the dorsal spinal cord to the floor plate (blue) in $Flk1^{CN\text{-}wt}$ embryos. Right: in $Flk1^{CN\text{-}ko}$ embryos, axons project in a highly disorganized and defasciculated manner and invade the motor columns.

(H) Left: histogram shows the quantification of the area occupied by commissural axons (% of the total spinal cord area, mean ± SEM). *p = 0.03, Student's t test; n = 5 $Flk1^{CN\text{-}wt}$; n = 8 $Flk1^{CN\text{-}ko}$. Right: histogram showing the penetrance of the phenotype (%); n = 13 $Flk1^{CN\text{-}wt}$; n = 12 $Flk1^{CN\text{-}ko}$. Differences in the penetrance of the phenotype between $Flk1^{CN\text{-}wt}$ and $Vegf^{FP\text{-}wt}$ might be due to their different genetic background. Scale bars represent 10 μm (A–C); 20 μm (D–F).

10–20 μm thickness. Purified commissural neurons were fixed in 4% PFA for 15 min on ice before processed for immunostaining. Dorsal spinal cord explants were fixed in 4% PFA overnight at 4°C. For immunohistochemistry, the following antibodies were used: anti-β-galactosidase (Cappel-55976), anti-CD31 (PharMingen-557355), anti-TAG-1 (clone 4D7, Developmental studies Hybridoma bank, DSHB), anti-Flk1 (Santa-Cruz, SC-6251 and SC-504), and anti-Robo3 (R&D systems, AF3076). Sections were subsequently incubated with fluorescently conjugated secondary antibodies (Molecular Probes, Alexa-488 or -546) for anti-TAG-1 and anti-Robo3, or with peroxidase-labeled IgGs (Dako), followed by amplification with tyramide-signal-amplification-system (Cy3-PerkinElmer-LifeSciences or FT-PerkinElmer-Life Sciences) for anti-GFP, anti-Flk1 (SC504) and anti-β-galactosidase. For immunostaining with anti-Flk1 (SC-6251), sections were subsequently incubated with peroxidase-labeled IgGs followed by amplification with Envision+System-HRP Labeled Polymer Anti-Mouse (Dako, K4000). Immunostainings were examined using Imager Z1 and Axioplan 2, and Axiovert 200M. Zeiss microscopes equipped with epifluorescence illumination or confocal system (Zeiss multiphoton CLSM510 Meta NLO, 0.5–1.0 μm optical sections).

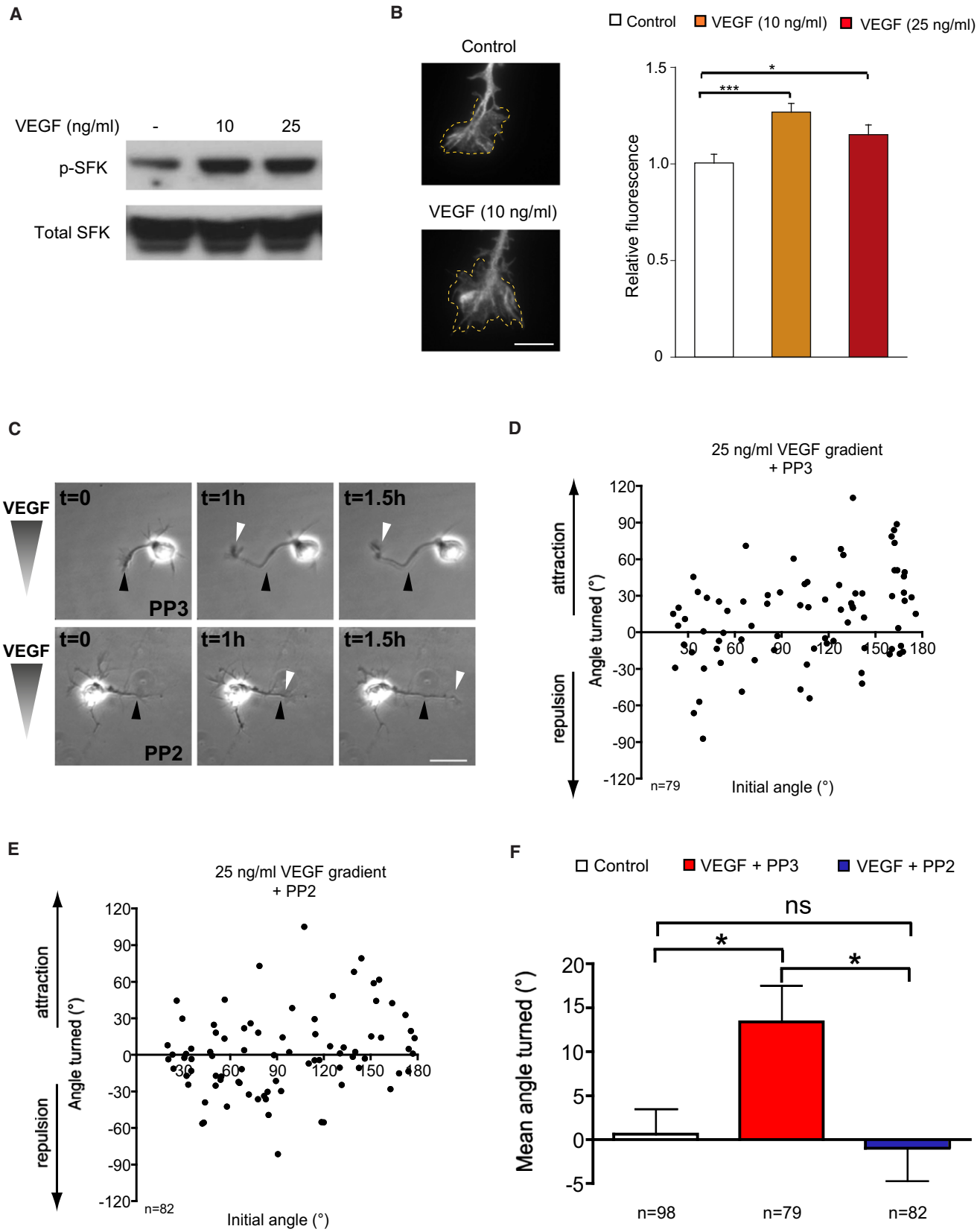
A
VEGF (ng/ml) - 10 25
p-SFK
Total SFK
B
Control
VEGF (10 ng/ml)
Control
VEGF (10 ng/ml)
VEGF (25 ng/ml)
Relative fluorescence
1.5
1.0
0.5
0
*
***
C
VEGF
t=0
t=1h
t=1.5h
PP3
VEGF
t=0
t=1h
t=1.5h
PP2
D
25 ng/ml VEGF gradient
+ PP3
attraction
repulsion
Angle turned (°)
120
90
60
30
0
-30
-60
-90
-120
30
60
90
120
150
180
n=79
Initial angle (°)
E
25 ng/ml VEGF gradient
+ PP2
attraction
repulsion
Angle turned (°)
120
90
60
30
0
-30
-60
-90
-120
30
60
90
120
150
180
n=82
Initial angle (°)
F
Control
VEGF + PP3
VEGF + PP2
ns
*
*
Mean angle turned (°)
20
15
10
5
0
-5
n=98
n=79
n=82

In Situ Hybridization

VEGF, Netrin-1, Shh, VEGF-C, Sema3E, Npn1, sense, and antisense riboprobes were DIG labeled by in vitro transcription (Roche) of cDNA encoding for their respective sequences. In situ hybridization in embryo cryosections was carried out as described in Marillat et al. (2002).

β-Gal Enzymatic Staining

E11.5 VEGF^{LacZ} embryos were fixed for 30 min in 0.2% glutaraldehyde in PBS buffered containing 2 mM $MgCl_2$ and 5 mM EGTA. After rinse, samples were embedded in 5% agarose and 100 μm vibratome floating sections were made. β-gal enzymatic activity was revealed with a developing solution containing 1 mg/ml X-gal (Invitrogen), 5 mM $K_4[Fe(CN)_6]$, and 5 mM $K_3[Fe(CN)_6]$.

Dunn Chamber Axon Guidance Assay and Analysis

Dunn chamber axon guidance assay was performed and analyzed as described (Yam et al., 2009). After Dunn chamber assembly and addition of VEGF, Sema3E, or VEGF-C (all at 25 ng/ml) to the outer well, time-lapse phase contrast images were acquired for 1.5 hr. Neutralizing anti-Flk1 (DC101) and anti-Npn1 (R&D systems, #AF566) antibodies were used at 100 ng/ml and 10 μg/ml, respectively. PP2 and PP3 (Calbiochem) were applied to the bath at a concentration of 800 nM. The angle turned was defined as the angle between the original direction of the axon and a straight line connecting the base of the growth cone from the first to the last time point of the assay period.

SFK and Phospho-SFK Immunostaining and Immunoblotting

Commissural neurons were cultured for 24 hr in vitro and subsequently stimulated with VEGF (10 or 25 ng/ml, R&D systems, #493-MV) for 30 min. For immunostaining, neurons were fixed in 4% PFA/4% sucrose (complemented with proteinase and phosphatase inhibitors [Roche]) for 15 min at room temperature. Immunostaining for P-SFK was performed using a Rabbit (polyclonal) anti-Src (pY418) phosphorylation site specific antibody (Invitrogen, #44660G) followed by an Alexa-488 conjugated secondary antibody. For immunoblotting, neurons were lysed in RIPA buffer complemented with proteinase and phosphatase inhibitors (Roche). An anti-Phospho-Src Family antibody (Cell Signaling, #2101) was used to probe the western blots. Subsequently blots were stripped and reprobed with an anti-Src (36D10) antibody (Cell Signaling, #2109).

Quantification of Phospho-SFK Fluorescence at Growth Cones

The average of the phospho-SFK fluorescence signal was measured for each growth cone using Image J and normalized to the average fluorescence signal in control growth cones. At least 50 growth cones were analyzed in two independent experiments (performed in triplicates) and statistical differences were assessed by unpaired t test versus control conditions.

Quantification of VEGF, Flk1, and Shh protein levels by ELISA

Floor plates (FPs) isolated from E11.5 mouse embryos were cultured in three dimensional rat tail collagen in B27-supplemented Neurobasal medium. Conditioned medium from FPs (explants from a single FP were cultured in 300 μl) or control medium were collected after 48 hr and processed for further measurements of VEGF and Shh protein concentration using the commercial Quantikine human VEGF ELISA kit (R&D Systems) and Shh ELISA kit (Abcam, ab100639), respectively. Flk1 protein expression was determined in lysates of E13 rat dorsal spinal cord tissue using the commercial mouse Flk1 ELISA kit (R&D Systems, Quantikine MVR200B).

Quantitative Real-Time RT-PCR

Expression levels were quantified by real-time RT-PCR, relative to the expression level of β-actin, using the following forward (F) and reverse primers (R) and probes (P), labeled with fluorescent dye (FAM) and quencher (TAMRA). *β-actin*: F,5′-AGAGGGAAATCGTGCGTGAC-3′; R,5′-CAATAGTGATGACCTGGCCGT-3′; P,5′-FAMCACTGCCGCATCCTCTTCCTCCCTAMRA-3′; *Flk1*: F,5′-ACTGCAGTGATTGCCATGTTCT-3′ ; R,5′-TCATTGGCCCGCTTAACG-3′; P,5′-FAMTGGCTCCTTCTTGTCATTGTCCTACGGATAMRA-3′; *Vegf*: F,5′-AGTCCCATGAAGTGATCAAGTTCA-3′; R,5′-ATCCGCATGATCTGCATGG-3′; P,5′-FAMTGCCCACGTCAGAGAGCAACATCACTAMRA-3′. Reference numbers for primer sequences for mShh and mNetrin-1 are Mm00436528_m1 and Mm00500896_m1, respectively (Applied Biosystems).

Quantification of the Area Occupied by Commissural Axons

The percentage of the area occupied by precrossing commissural axons to the total spinal cord area was quantified based on a previously described method (Charron et al., 2003). Briefly, precrossing commissural axon area and total spinal cord area were measured on E11.5 embryo cross-sections by quantifying the area encompassed by Robo-3$^+$ axons and the edges of the spinal cord, respectively. Measurements were performed using the NIH Image J software. Values were normalized to values obtained for the control group for each litter.

Collagen Outgrowth Assays

E13 rat dorsal spinal cord explants were dissected and embedded in three-dimensional collagen matrices as described (Charron et al., 2003) and cultured in F12:DMEM (1:1), 10% heat-inactivated horse serum, 40 mM glucose, 2 mM glutaMAX, 100 μg/ml streptomycin sulfate, and 100 U/ml penicillin for 16 hr. Where indicated, Netrin-1 (50 or 100 ng/ml) or VEGF (10, 50, or 100 ng/ml) were added to the medium.

Quantification of Commissural Axon Outgrowth in Explants

Commissural axons were detected by TAG-1 immunostaining and the total length of axon bundles per explant (for outgrowth) was quantified as described previously (Charron et al., 2003).

SUPPLEMENTAL INFORMATION

Supplemental Information includes four figures and one movie and can be found with this article online at doi:10.1016/j.neuron.2011.04.014.

Figure 6. VEGF-Induced Growth Cone Turning Requires SFK Activation

(A) Immunoblot for anti-phospho-SFK (Y418) (top) and total SFK (bottom) of dissociated rat commissural neurons incubated with 0, 10, or 25 ng/ml of VEGF for 30 min.

(B) Dissociated rat commissural neurons were incubated with vehicle (control) (top) or 10 ng/ml of VEGF (bottom) for 30 min, and then fixed and immunostained with anti-phospho-SFK (Y418). Dotted lines delineate growth cones. VEGF stimulation leads to an increase in phospho-SFKs in the growth cone. Graph: mean relative levels (±SEM) of phospho-SFK fluorescence in control and VEGF-stimulated (10 or 25 ng/ml) growth cones. The average phospho-SFK fluorescence signal was measured for each growth cone and normalized to the mean signal in control-stimulated growth cones. n = 129 for control, n = 167 for VEGF (10 ng/ml) and n = 107 for VEGF (25 ng/ml), were measured in two independent experiments. ***$p < 0.0001$; *$p < 0.05$ (unpaired t test).

(C) Axons of dissociated commissural neurons in a 25 ng/ml VEGF gradient in a Dunn chamber, in the presence of bath-applied PP2 (0.8 μM) or PP3 (0.8 μM). Inhibition of SFK activity by PP2 inhibits VEGF-mediated turning. PP3 did not inhibit the ability of axons to turn up a VEGF gradient. Black arrowhead points to the initial position of the growth cone; white arrowhead points to its final position.

(D–F) Scatter plot of the angle turned versus initial angle (D and E) and mean angle turned (F) (±SEM) for initial angles >20°, show that SFK inhibition by PP2 (E and F), but not by PP3 (D and F), inhibits commissural axon turning toward VEGF ($p < 0.05$; $p = 0.73$, respectively, in unpaired t test). Axon turning up a VEGF gradient is not perturbed by PP3 and was significantly different from the control or the PP2 condition ($p < 0.05$, initial angle >20°); one-way ANOVA with Bonferroni multiple comparison post-test, *$p < 0.05$; ns: not significant. Scale bars represent 10 μm (B); 20 μm (C).

ACKNOWLEDGMENTS

We thank D. Schmucker and L. Moons for helpful advice and discussions, A. McMahon (Harvard University) for providing the Wnt1-Cre mouse line to A.C., A. Nagy for providing the VEGF^{LacZ} mice, D. Anderson for providing the VEGF$^{lox/lox}$ mice, and C. Henderson for providing the Sema3E probe for ISH. The authors also thank N. Dai, M. De Mol, A. Manderveld, B. Vanwetswinkel, K. Peeters, L. Goddé, A. Bouché, P. Vanwesemael, J. Van Dijck, S. Morin, and P.T. Yam for assistance. This study was supported by "Long-term structural Methusalem funding by the Flemish Government," the Fund for Scientific Research-Flemish Government (FWO) (G.0319.07, G.0677.09, G.02010.07, G.0676.09, 1.5.210.10.N.00 [Krediet aan navorsers]), Concerted Research Activities K.U. Leuven (GOA/2006/11), and the Belgian Science Policy (IUAP-P6/20 and IUAP-P6/30), the Association Française contre les myopathies (AFM), Geneeskundige stichting Koningin Elisabeth, and MND/A grant 70/130. C.R.A. is postdoctoral fellow of the FWO (1.2.545.09.N.00, V.4.332.10.N.01). C.C. is a fellow of the Flemish Institute for the promotion of scientific research (IWT), Belgium. I.S. is a postdoctoral fellow of the European Union Seventh framework program. C.L. is supported by an EMBO long-term postdoctoral fellowship. A.C. is supported by grants from the "Fondation pour la recherche médicale" (programme Equipe FRM) and the Agence Nationale de la Recherche (ANR-08-MNPS-030-01). F.C. is a Fonds de la recherche en santé du Québec (FRSQ) Scientist. Work performed in the Charron laboratory was supported by an operating grant from the Canadian Institutes of Health Research (CIHR).

Accepted: April 15, 2011
Published: June 8, 2011

REFERENCES

Avantaggiato, V., Orlandini, M., Acampora, D., Oliviero, S., and Simeone, A. (1998). Embryonic expression pattern of the murine figf gene, a growth factor belonging to platelet-derived growth factor/vascular endothelial growth factor family. Mech. Dev. *73*, 221–224.

Baldwin, M.E., Catimel, B., Nice, E.C., Roufail, S., Hall, N.E., Stenvers, K.L., Karkkainen, M.J., Alitalo, K., Stacker, S.A., and Achen, M.G. (2001). The specificity of receptor binding by vascular endothelial growth factor-d is different in mouse and man. J. Biol. Chem. *276*, 19166–19171.

Bellon, A., Luchino, J., Haigh, K., Rougon, G., Haigh, J., Chauvet, S., and Mann, F. (2010). VEGFR2 (KDR/Flk1) signaling mediates axon growth in response to semaphorin 3E in the developing brain. Neuron *66*, 205–219.

Böcker-Meffert, S., Rosenstiel, P., Röhl, C., Warneke, N., Held-Feindt, J., Sievers, J., and Lucius, R. (2002). Erythropoietin and VEGF promote neural outgrowth from retinal explants in postnatal rats. Invest. Ophthalmol. Vis. Sci. *43*, 2021–2026.

Carmeliet, P., Ferreira, V., Breier, G., Pollefeyt, S., Kieckens, L., Gertsenstein, M., Fahrig, M., Vandenhoeck, A., Harpal, K., Eberhardt, C., et al. (1996). Abnormal blood vessel development and lethality in embryos lacking a single VEGF allele. Nature *380*, 435–439.

Charron, F., and Tessier-Lavigne, M. (2005). Novel brain wiring functions for classical morphogens: a role as graded positional cues in axon guidance. Development *132*, 2251–2262.

Charron, F., Stein, E., Jeong, J., McMahon, A.P., and Tessier-Lavigne, M. (2003). The morphogen sonic hedgehog is an axonal chemoattractant that collaborates with netrin-1 in midline axon guidance. Cell *113*, 11–23.

Chen, H., Chédotal, A., He, Z., Goodman, C.S., and Tessier-Lavigne, M. (1997). Neuropilin-2, a novel member of the neuropilin family, is a high affinity receptor for the semaphorins Sema E and Sema IV but not Sema III. Neuron *19*, 547–559.

Cheng, L., Jia, H., Löhr, M., Bagherzadeh, A., Holmes, D.I., Selwood, D., and Zachary, I. (2004). Anti-chemorepulsive effects of vascular endothelial growth factor and placental growth factor-2 in dorsal root ganglion neurons are mediated via neuropilin-1 and cyclooxygenase-derived prostanoid production. J. Biol. Chem. *279*, 30654–30661.

Dickson, B.J., and Zou, Y. (2010). Navigating intermediate targets: the nervous system midline. Cold Spring Harb Perspect Biol. *2*, a002055.

Eliceiri, B.P., Puente, X.S., Hood, J.D., Stupack, D.G., Schlaepfer, D.D., Huang, X.Z., Sheppard, D., and Cheresh, D.A. (2002). Src-mediated coupling of focal adhesion kinase to integrin alpha(v)beta5 in vascular endothelial growth factor signaling. J. Cell Biol. *157*, 149–160.

Ema, M., Takahashi, S., and Rossant, J. (2006). Deletion of the selection cassette, but not cis-acting elements, in targeted Flk1-lacZ allele reveals Flk1 expression in multipotent mesodermal progenitors. Blood *107*, 111–117.

Ferrara, N., Carver-Moore, K., Chen, H., Dowd, M., Lu, L., O'Shea, K.S., Powell-Braxton, L., Hillan, K.J., and Moore, M.W. (1996). Heterozygous embryonic lethality induced by targeted inactivation of the VEGF gene. Nature *380*, 439–442.

Gerber, H.P., Hillan, K.J., Ryan, A.M., Kowalski, J., Keller, G.A., Rangell, L., Wright, B.D., Radtke, F., Aguet, M., and Ferrara, N. (1999). VEGF is required for growth and survival in neonatal mice. Development *126*, 1149–1159.

Haigh, J.J., Morelli, P.I., Gerhardt, H., Haigh, K., Tsien, J., Damert, A., Miquerol, L., Muhlner, U., Klein, R., Ferrara, N., et al. (2003). Cortical and retinal defects caused by dosage-dependent reductions in VEGF-A paracrine signaling. Dev. Biol. *262*, 225–241.

Hogan, K.A., Ambler, C.A., Chapman, D.L., and Bautch, V.L. (2004). The neural tube patterns vessels developmentally using the VEGF signaling pathway. Development *131*, 1503–1513.

James, J.M., Gewolb, C., and Bautch, V.L. (2009). Neurovascular development uses VEGF-A signaling to regulate blood vessel ingression into the neural tube. Development *136*, 833–841.

Jin, K., Zhu, Y., Sun, Y., Mao, X.O., Xie, L., and Greenberg, D.A. (2002). Vascular endothelial growth factor (VEGF) stimulates neurogenesis in vitro and in vivo. Proc. Natl. Acad. Sci. USA *99*, 11946–11950.

Karkkainen, M.J., Haiko, P., Sainio, K., Partanen, J., Taipale, J., Petrova, T.V., Jeltsch, M., Jackson, D.G., Talikka, M., Rauvala, H., et al. (2004). Vascular endothelial growth factor C is required for sprouting of the first lymphatic vessels from embryonic veins. Nat. Immunol. *5*, 74–80.

Kennedy, T.E., Wang, H., Marshall, W., and Tessier-Lavigne, M. (2006). Axon guidance by diffusible chemoattractants: a gradient of netrin protein in the developing spinal cord. J. Neurosci. *26*, 8866–8874.

Langlois, S.D., Morin, S., Yam, P.T., and Charron, F. (2010). Dissection and culture of commissural neurons from embryonic spinal cord. J. Vis. Exp. (39) 10.3791/1773.

Li, X., and Lufkin, T. (2000). Cre recombinase expression in the floorplate, notochord and gut epithelium in transgenic embryos driven by the Hoxa-1 enhancer III. Genesis *26*, 121–122.

Li, W., Lee, J., Vikis, H.G., Lee, S.H., Liu, G., Aurandt, J., Shen, T.L., Fearon, E.R., Guan, J.L., Han, M., et al. (2004). Activation of FAK and Src are receptor-proximal events required for netrin signaling. Nat. Neurosci. *7*, 1213–1221.

Liu, G., Beggs, H., Jürgensen, C., Park, H.T., Tang, H., Gorski, J., Jones, K.R., Reichardt, L.F., Wu, J., and Rao, Y. (2004). Netrin requires focal adhesion kinase and Src family kinases for axon outgrowth and attraction. Nat. Neurosci. *7*, 1222–1232.

Liu, G., Li, W., Gao, X., Li, X., Jürgensen, C., Park, H.T., Shin, N.Y., Yu, J., He, M.L., Hanks, S.K., et al. (2007). p130CAS is required for netrin signaling and commissural axon guidance. J. Neurosci. *27*, 957–968.

Lohela, M., Bry, M., Tammela, T., and Alitalo, K. (2009). VEGFs and receptors involved in angiogenesis versus lymphangiogenesis. Curr. Opin. Cell Biol. *21*, 154–165.

Maes, C., Goossens, S., Bartunkova, S., Drogat, B., Coenegrachts, L., Stockmans, I., Moermans, K., Nyabi, O., Haigh, K., Naessens, M., et al. (2010). Increased skeletal VEGF enhances beta-catenin activity and results in excessively ossified bones. EMBO J. *29*, 424–441.

Marillat, V., Cases, O., Nguyen-Ba-Charvet, K.T., Tessier-Lavigne, M., Sotelo, C., and Chédotal, A. (2002). Spatiotemporal expression patterns of slit and robo genes in the rat brain. J. Comp. Neurol. *442*, 130–155.

Marko, S.B., and Damon, D.H. (2008). VEGF promotes vascular sympathetic innervation. Am. J. Physiol. Heart Circ. Physiol. *294*, H2646–H2652.

Meriane, M., Tcherkezian, J., Webber, C.A., Danek, E.I., Triki, I., McFarlane, S., Bloch-Gallego, E., and Lamarche-Vane, N. (2004). Phosphorylation of DCC by Fyn mediates Netrin-1 signaling in growth cone guidance. J. Cell Biol. *167*, 687–698.

Miquerol, L., Gertsenstein, M., Harpal, K., Rossant, J., and Nagy, A. (1999). Multiple developmental roles of VEGF suggested by a LacZ-tagged allele. Dev. Biol. *212*, 307–322.

Miquerol, L., Langille, B.L., and Nagy, A. (2000). Embryonic development is disrupted by modest increases in vascular endothelial growth factor gene expression. Development *127*, 3941–3946.

Nagase, T., Nagase, M., Yoshimura, K., Fujita, T., and Koshima, I. (2005). Angiogenesis within the developing mouse neural tube is dependent on sonic hedgehog signaling: possible roles of motor neurons. Genes Cells *10*, 595–604.

Okada, A., Charron, F., Morin, S., Shin, D.S., Wong, K., Fabre, P.J., Tessier-Lavigne, M., and McConnell, S.K. (2006). Boc is a receptor for sonic hedgehog in the guidance of commissural axons. Nature *444*, 369–373.

Olsson, A.K., Dimberg, A., Kreuger, J., and Claesson-Welsh, L. (2006). VEGF receptor signalling—in control of vascular function. Nat. Rev. *7*, 359–371.

Oosthuyse, B., Moons, L., Storkebaum, E., Beck, H., Nuyens, D., Brusselmans, K., Van Dorpe, J., Hellings, P., Gorselink, M., Heymans, S., et al. (2001). Deletion of the hypoxia-response element in the vascular endothelial growth factor promoter causes motor neuron degeneration. Nat. Genet. *28*, 131–138.

Robles, E., Woo, S., and Gomez, T.M. (2005). Src-dependent tyrosine phosphorylation at the tips of growth cone filopodia promotes extension. J. Neurosci. *25*, 7669–7681.

Roelink, H., Porter, J.A., Chiang, C., Tanabe, Y., Chang, D.T., Beachy, P.A., and Jessell, T.M. (1995). Floor plate and motor neuron induction by different concentrations of the amino-terminal cleavage product of sonic hedgehog autoproteolysis. Cell *81*, 445–455.

Rosenstein, J.M., Krum, J.M., and Ruhrberg, C. (2010). VEGF in the nervous system. Organogenesis *6*, 107–114.

Rosenstein, J.M., Mani, N., Khaibullina, A., and Krum, J.M. (2003). Neurotrophic effects of vascular endothelial growth factor on organotypic cortical explants and primary cortical neurons. J. Neurosci. *23*, 11036–11044.

Ruiz de Almodovar, C., Coulon, C., Salin, P.A., Knevels, E., Chounlamountri, N., Poesen, K., Hermans, K., Lambrechts, D., Van Geyte, K., Dhondt, J., et al. (2010). Matrix-binding vascular endothelial growth factor (VEGF) isoforms guide granule cell migration in the cerebellum via VEGF receptor Flk1. J. Neurosci. *30*, 15052–15066.

Ruiz de Almodovar, C., Lambrechts, D., Mazzone, M., and Carmeliet, P. (2009). Role and therapeutic potential of VEGF in the nervous system. Physiol. Rev. *89*, 607–648.

Schwarz, Q., Gu, C., Fujisawa, H., Sabelko, K., Gertsenstein, M., Nagy, A., Taniguchi, M., Kolodkin, A.L., Ginty, D.D., Shima, D.T., and Ruhrberg, C. (2004). Vascular endothelial growth factor controls neuronal migration and cooperates with Sema3A to pattern distinct compartments of the facial nerve. Genes Dev. *18*, 2822–2834.

Schwarz, Q., and Ruhrberg, C. (2010). Neuropilin, you gotta let me know: should I stay or should I go? Cell Adh. Migr. *4*, 61–66.

Schwarz, Q., Waimey, K.E., Golding, M., Takamatsu, H., Kumanogoh, A., Fujisawa, H., Cheng, H.J., and Ruhrberg, C. (2008). Plexin A3 and plexin A4 convey semaphorin signals during facial nerve development. Dev. Biol. *324*, 1–9.

Serafini, T., Colamarino, S.A., Leonardo, E.D., Wang, H., Beddington, R., Skarnes, W.C., and Tessier-Lavigne, M. (1996). Netrin-1 is required for commissural axon guidance in the developing vertebrate nervous system. Cell *87*, 1001–1014.

Soker, S., Takashima, S., Miao, H.Q., Neufeld, G., and Klagsbrun, M. (1998). Neuropilin-1 is expressed by endothelial and tumor cells as an isoform-specific receptor for vascular endothelial growth factor. Cell *92*, 735–745.

Sondell, M., and Kanje, M. (2001). Postnatal expression of VEGF and its receptor flk-1 in peripheral ganglia. Neuroreport *12*, 105–108.

Sondell, M., Lundborg, G., and Kanje, M. (1999). Vascular endothelial growth factor has neurotrophic activity and stimulates axonal outgrowth, enhancing cell survival and Schwann cell proliferation in the peripheral nervous system. J. Neurosci. *19*, 5731–5740.

Storkebaum, E., Lambrechts, D., Dewerchin, M., Moreno-Murciano, M.P., Appelmans, S., Oh, H., Van Damme, P., Rutten, B., Man, W.Y., De Mol, M., et al. (2005). Treatment of motoneuron degeneration by intracerebroventricular delivery of VEGF in a rat model of ALS. Nat. Neurosci. *8*, 85–92.

Storkebaum, E., Ruiz de Almodovar, C., Meens, M., Zacchigna, S., Mazzone, M., Vanhoutte, G., Vinckier, S., Miskiewicz, K., Poesen, K., Lambrechts, D., et al. (2010). Impaired autonomic regulation of resistance arteries in mice with low vascular endothelial growth factor or upon vascular endothelial growth factor trap delivery. Circulation *122*, 273–281.

Tam, S.J., and Watts, R.J. (2010). Connecting vascular and nervous system development: angiogenesis and the blood-brain barrier. Annu. Rev. Neurosci. *33*, 379–408.

Wittko, I.M., Schänzer, A., Kuzmichev, A., Schneider, F.T., Shibuya, M., Raab, S., and Plate, K.H. (2009). VEGFR-1 regulates adult olfactory bulb neurogenesis and migration of neural progenitors in the rostral migratory stream in vivo. J. Neurosci. *29*, 8704–8714.

Yam, P.T., Langlois, S.D., Morin, S., and Charron, F. (2009). Sonic hedgehog guides axons through a noncanonical, Src-family-kinase-dependent signaling pathway. Neuron *62*, 349–362.

Zacchigna, S., Ruiz de Almodovar, C., and Carmeliet, P. (2008). Similarities between angiogenesis and neural development: what small animal models can tell us. Curr. Top. Dev. Biol. *80*, 1–55.

Zhang, H., Vutskits, L., Pepper, M.S., and Kiss, J.Z. (2003). VEGF is a chemoattractant for FGF-2-stimulated neural progenitors. J. Cell Biol. *163*, 1375–1384.

Zou, Y., Stoeckli, E., Chen, H., and Tessier-Lavigne, M. (2000). Squeezing axons out of the gray matter: a role for slit and semaphorin proteins from midline and ventral spinal cord. Cell *102*, 363–375.